The Mechanism of Jet Entrainment

K. Bremhorst*
University of Queensland, Brisbane, Australia
and
W. H. Harch†
Aeronautical Research Laboratories, Melbourne, Australia

I. Introduction

CONSIDERABLE research effort is being exerted to develop jet flows with higher entrainment than encountered in steady jets. Such efforts are highly empirical as the basic entrainment mechanism is not well understood. It is generally accepted that irrotational fluid which acquires vorticity is said to have been entrained. The entrainment process is, therefore, one of vorticity propagation by viscous action. Controversy exists, however, concerning the manner in which this takes place,[1] although the general belief is that the large structure of the turbulent/nonturbulent interface is a significant factor in the whole process.[1-3]

Comparison of different types of flows to permit conclusions concerning the effect of flow structure on entrainment is difficult, but some qualitative differences between the large interfacial structures for wakes and boundary layers to account for their different entrainment characteristics have been postulated.[2] Recently reported measurements[4] show that the entrainment and entrainment rate of a fully pulsed subsonic air jet are considerably higher than for a steady jet. The physical reasons for such an increase have not been shown so far, but are now believed to be due to a significant increase in the size of the jet structure consequent upon the pulsation.

II. Pulsed Jet Description

The fully pulsed jet to be considered was produced by a rotating valve[4] which opened for one-third of each revolution so that pulses of fluid were well separated from neighboring upstream and downstream ones. A typical hot-wire signal obtained at some downstream point is sketched in Fig. 1. For a fully pulsed jet, $t_1 \leq t_p$. The time mean velocity U at the jet exit was 36.6 m/s. U_p is the periodic or total pseudoturbulence component of the signal obtained by ensemble-averaging the total instantaneous velocity, U_i, over many cycles at time τ_p from the beginning of the pulsating cycle. Fluctuating velocities of much higher frequency than the frequency of pulsation are found superimposed on the pseudoturbulence component. These constitute the intrinsic turbulence u' which, combined with the pseudoturbulence u_p, results in the total or aggregate turbulence, u. Since τ_p was measured relative to the time of valve opening, it follows that the intrinsic turbulence includes all shear-generated turbulence as well as any unsteadiness associated with the pseudoturbulence.

A shaping orifice of 25.4-mm diam d was placed at the jet exit to ensure axisymmetric flow and to give a fixed exit size. Flow Strouhal numbers St based on this diameter, the mean exit velocity, and frequency of pulsation were 0.0071 (10 Hz tests) and 0.0176 (25 Hz tests). These Strouhal numbers are well below the natural Strouhal number ($St \simeq 0.3$) of steady jets,[5] so that many of the jet's characteristics can be expected

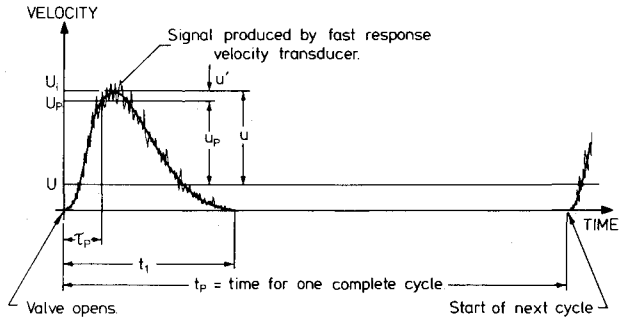

Fig. 1 Typical instantaneous velocity signal in a fully pulsed jet.

to resemble those of steady jets. It is not surprising then that the radial and axial intrinsic turbulence intensity distributions for a large part of the flow are identical to those of steady jets.[4] A similar equivalence has been observed for basic statistical parameters such as the skewness and flatness of the intrinsic turbulence. A noticeable exception to this, however, is the region within ten exit diameters from the jet exit where the intrinsic turbulence for the fully pulsed jet is significantly higher than for its steady counterpart.

III. Correlation Measurements in a Pulsed Jet

Space-time correlations are required for the accurate measurement of spatial structure of a nonfrozen, turbulent field. If Taylor's hypothesis can be applied, it is sufficient to measure single-point autocorrelations from which spatial information can be inferred if the local mean velocity is known. At the interface between turbulent and nonturbulent fluid it is known that Taylor's hypothesis breaks down, but the difference between the convection velocity of the turbulent field and the local mean velocity is not large.[3,6] For indicative results, the use of Taylor's hypothesis is, therefore, a reasonable approximation. Furthermore, if it is assumed that the bulk of the entrainment is due to the propagation of vorticity by the intrinsic turbulence, only this component is of further interest. Such an assumption is justified as the pseudoturbulence component is likely to introduce only irrotational fluctuations which are not part of the entrained flow.

For the pulsed jet intrinsic turbulence, the nonstationary autocorrelation coefficient defined by

$$R_{11}(\tau_p,\tau) = \frac{\overline{u'(\tau_p)u'(\tau_p+\tau)}}{[u'^2(\tau_p)\;u'^2(\tau_p+\tau)]^{1/2}} \tag{1}$$

must be introduced due to the presence of the pseudoturbulence component.

Alternatively, this can be rewritten as

$$R_{11}(\tau_p,\tau) = \left[\frac{\overline{u'^2(\tau_p)}/U_p^2(\tau_p)}{u'^2(\tau_p+\tau)/U_p^2(\tau_p+\tau)}\right]^{1/2} \times \left[\frac{U_p(\tau_p)}{U_p(\tau_p+\tau)}\right] R'_{11}(\tau_p,\tau) \tag{2}$$

where

$$R'_{11}(\tau_p,\tau) = \frac{\overline{u'(\tau_p)u'(\tau_p+\tau)}}{\overline{u'^2(\tau_p)}} \tag{3}$$

For stationary signals, $R'_{11}(\tau_p,\tau)$ becomes independent of τ_p.

Measurements[4] indicate that for the pulsed jet $\overline{u'^2(\tau_p)}/U_p^2(\tau_p)$ is nearly independent of τ_p, particularly after the peak velocity point in the cycle, so that Eq. (2) reduces to

$$R_{11}(\tau_p,\tau) \simeq [U_p(\tau_p)/U_p(\tau_p+\tau)]R'_{11}(\tau_p,\tau) \tag{4}$$

Received April 10, 1978; revision received June 2, 1978.

Index categories: Nonsteady Aerodynamics; Jets, Wakes, and Viscid-Inviscid Flow Interactions.

*Senior Lecturer, Dept. of Mechanical Engineering.
†Experimental Officer, Dept. of Defence.

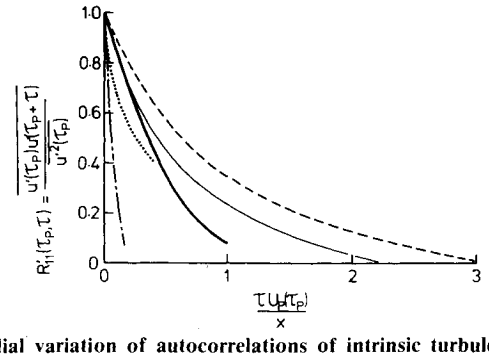

a) Radial variation of autocorrelations of intrinsic turbulence. For fully pulsed jet,[7] $x/d=7$, $St=0.0176$: ——$r/r_{1/2}=0$, – – – $r/r_{1/2}=0.8$, ——— $r/r_{1/2}=1.6$.

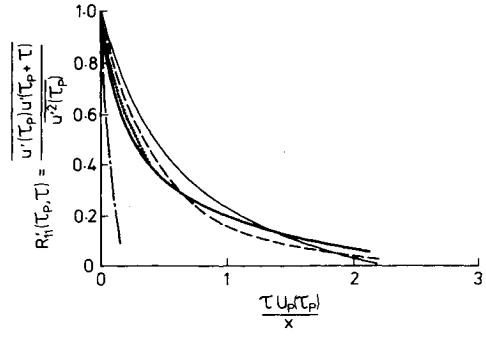

b) Axial variation of autocorrelations of intrinsic turbulence at $r/r_{1/2}=0$. For fully pulsed jet,[7] $St=0.0176$: ——$x/d=7$, – – – $x/d=11$, ——— $x/d=17$.

Fig. 2 Far field, steady round jet[6]: —·—·—. Mixing region of steady plane jet[8] (moving axis autocorrelation) · · ·.

Furthermore, for values of τ of interest, where $R_{11}(\tau_p,\tau)$ is significantly greater than zero, it is found that $\tau \ll t_1$ and $U_p(\tau_p) \simeq U_p(\tau_p+\tau)$ so that $R_{11}(\tau_p,\tau) \simeq R^1{}_{11}(\tau_p,\tau)$. When replacing the time delay, τ, with the normalized one $\tau U_p(\tau_p)/x$, it is found that in the far-field region of steady jets $R^1{}_{11}(\tau_p, \tau U_p(\tau_p)/x)$ is independent of τ_p and is also self-preserving.[6]

Measurements of $R^1{}_{11}(\tau_p,\tau U_p(\tau_p)/x)$ were made in the fully pulsed jet using a hot-wire anemometer and an EAI Pacer 600 hybrid computer for subsequent signal analysis.[7] Typical results are shown in Figs. 2a and 2b where x is the distance from the exit orifice. $R^1{}_{11}(\tau_p,\tau U_p(\tau_p)/x)$ was found to be almost independent of τ_p in the region of the signal after the peak U_p. Similar data obtained at $x/d=11$ and 17, Fig. 2b, indicate that normalization of τ with $(x+a)$ instead of x collapses onto a single curve the results at different x/d for $\tau U_p(\tau_p)/x<0.5$ when $a=9.4d$. This value of effective origin of the intrinsic turbulence agrees with that obtained for the mean velocity field. Results at $St=0.0071$ are similar to those of Figs. 2a and 2b.

Comparison with correlations in steady jets shows that time scales for the two types of jets differ by at least an order of magnitude. If Taylor's hypothesis is assumed to apply to a first approximation, significantly longer length scales are implied for the intrinsic turbulence of the pulsed jet. This component of the pulsed jet turbulence is primarily due to the action of shearing forces and could, therefore, be expected to be similar to the turbulence of steady jets. It is noteworthy that a change of scaling of the time delay to allow for the upstream shift of the effective origin has relatively little effect on the preceding conclusion; whereas the approximation introduced by use of $R^1{}_{11}(\tau_p,\tau)$ instead of $R_{11}(\tau_p,\tau)$ decreases the difference between the two types of jets hence yielding a conservative result. Another possible source of variation of Fig. 2 for the pulsed-jet correlations is the use of U_p instead of the average of U_p taken over the interval τ_p to $\tau_p+\tau$ as is required if Taylor's hypothesis applies. However, since $U_p(\tau_p)$ and $U_p(\tau_p+\tau)$ differ little over the highly correlated part of the delay interval no significant error results if $U_p(\tau_p)$ is used. Finally, if the true convection velocity is much larger than $U_p(\tau_p)$, better agreement between the steady jet and pulsed jet scales would be obtained, but this would be inconsistent with convection velocity measurements in steady jets for which the convection velocity is only twice the local mean velocity at the largest $r/r_{1/2}$ reported here.[6] For smaller radial distances the two velocities are almost equal.

Assuming that a large streamwise length scale in the bulk of the flow also implies a large lateral spread of the surface indentations, leads to the conclusion that the mean velocity profile should have a larger tail in this region. Comparison of steady jet radial mean velocity profiles[6] which are well represented by

$$U/U_0 = e^{-0.693(r/r_{1/2})^2} \tag{5a}$$

with fully pulsed jet profiles[4] represented by

$$U/U_0 = [1+0.44(r/r_{1/2})^2]^{-2} \tag{5b}$$

verifies this proposition. $r_{1/2}$ in these equations is the radial position, r, at which the mean streamwise velocity equals half the center-line value, U_0.

Unfortunately, direct comparison of the pulsed jet data is possible only with far-field steady data. However, if moving axis autocorrelations in the pulsed jet follow those in other flows,[8] then these will be much larger than the single-point autocorrelations of Fig. 2. It follows that such correlations would be much larger than similar ones obtained in steady mixing layers, Fig. 2, which is consistent with the preceding findings.

IV. Conclusion

Based on the assumption that entrainment of irrotational exterior fluid in pulsed jets is principally due to the intrinsic turbulence component, it may be concluded from autocorrelations of the intrinsic turbulence of fully pulsed jets that the size of the turbulent/nonturbulent interface indentations is significantly larger than for steady jets. In view of the generally accepted belief that the larger scale structure of this interface is related to the entrainment of irrotational exterior fluid, it is probable that the much larger entrainment of fully pulsed jets is a direct consequence of its larger entrainment interface structure.

Acknowledgments

The authors are grateful for support received from the Australian Research Grants Committee and to T. C. Smith for his assistance with the computations. The second author also gratefully acknowledges receipt of a Commonwealth Postgraduate Scholarship.

References

[1] Bevilaqua, P. M. and Lykoudis, P. S., "Some Observations on the Mechanism of Entrainment," *AIAA Journal*, Vol. 15, Aug. 1977, pp. 1194-1196.

[2] Townsend, A. A., "Entrainment and the Structure of Turbulent Flow," *Journal of Fluid Mechanics*, Vol. 41, 1970, pp. 13-46.

[3] Kovasznay, L. S. G., Kibens, V., and Blackwelder, R. F., "Large-Scale Motion in the Intermittent Region of a Turbulent Boundary Layer," *Journal of Fluid Mechanics*, Vol. 41, 1970, pp. 283-325.

[4] Bremhorst, K. and Harch, W. H., "Near Field Velocity Measurements in a Fully Pulsed Subsonic Air Jet," *Proceedings of the First Symposium on Turbulent Shear Flows*, April 1977, The Pennsylvania State University, University Park, Pa., Springer, to appear.

[5] Crow, S. C. and Champagne, F. H., "Orderly Structure in Jet Turbulence," *Journal of Fluid Mechanics*, Vol. 48, 1971, pp. 547-591.

[6]Wygnanski, I. and Fiedler, H. E., "Some Measurements in the Self-Preserving Jet," *Journal of Fluid Mechanics*, Vol. 38, 1969, pp. 577-612.

[7]Harch, W. H., "An Experimental Investigation Into the Velocity Field and Aerodynamic Noise Sources of an Unheated Fully Pulsed Air Jet," Ph.D. Thesis, University of Queensland, St. Lucia, Brisbane, Australia, 1977.

[8]Wygnanski, I. and Fiedler, H. W., "The Two-Dimensional Mixing Region," *Journal of Fluid Mechanics*, Vol. 41, 1970, pp. 327-361.

Resonance Refractivity Studies of Sodium Vapor for Enhanced Flow Visualization

G. Blendstrup* and D. Bershader†
Stanford University, Stanford, Calif.
and
P.W. Langhoff‡
Indiana University, Bloomington, Ind.

Introduction

REFRACTIVE methods pioneered by the studies of Mach, Zehnder, Toepler, and others have been used for about 100 years to visualize fluid-dynamic flow phenomena. While there have been new developments in sophistication of the optical methodology and instrumentation, the sensitivity of essentially all work to date has been controlled by the specific refractivity of diatomic gases, e.g., air, in the visible portion of the spectrum. That quantity, K_0, appears in the well-known Dale-Gladstone constitutive relation[1]

$$n-1=K_0\rho \tag{1}$$

relating refractive index n and gas density ρ. Its value is relatively constant over the visible portion of the spectrum:

$$K_{0_{\text{air}}} \approx 2.3\times 10^{-4}\ \text{m}^3/\text{kg}$$

The relatively small magnitude of $K_{0_{\text{air}}}$ has largely limited the application of techniques such as interferometry, Schlieren, and shadowgraphy to compressible flows with substantial density gradients; or to free convective flows with sizable thermal gradients. As an example, the density change corresponding to 0.1 fringe shift in a test rig with a transverse light path of 10 cm is 2.2×10^{-3} kg/m^3 or 0.17% of standard atmospheric density. It turns out that a substantially higher sensitivity is desirable for several applications of current interest. These include vortices and turbulence in low-speed flow, propagation of sound or noise in the audible range, rarified gas flow, and meteorological flows.

The idea of using a tunable narrow band dye laser to illuminate a gas near its resonance line in order to increase the effective Dale-Gladstone "constant" was discussed in an earlier paper by two of the present authors.[2] Since the resonance transitions of air and other diatomic gases lie in the far ultraviolet, the work just referred to as well as the present Note deals with the resonance refractivity of sodium vapor. In a laboratory application of this method, the working fluid would be seeded with small quantities of sodium vapor or other suitable material, probably in the range 10^{-4} to 10^{-3} mole fraction.

The present Note describes recent results, including refinement of both the theoretical calculations and the experimental setup to check the resonance dispersion of sodium vapor, as well as the final calibration experiment on sodium vapor refractivity.

Theoretical

Atomic absorption and dispersion line shapes under conditions of Doppler, collision, and natural broadening can be represented by Voigt profiles of the form[3]

$$n_r(\nu)-1=\frac{\sqrt{\ell n2}}{8\pi^2\sqrt{\pi}}\cdot\frac{e^2Nf_r}{m\epsilon_0\gamma_D\nu_r}\int_{-\infty}^{\infty}\frac{\epsilon-\nu}{(\epsilon-\nu)^2+\gamma_L^2/4}$$
$$\cdot\exp[-4\,\ell n2\cdot(\epsilon-\nu_r)^2/\gamma_D^2]\,d\epsilon \tag{2}$$

$$\mu_r(\nu)=\frac{\sqrt{\ell n2}}{4\pi\sqrt{\pi}}\cdot\frac{e^2Nf_r\gamma_L}{mc\epsilon_0\gamma_D}\int_{-\infty}^{\infty}\frac{1}{(\epsilon-\nu)^2+\gamma_L^2/4}$$
$$\cdot\exp[-4\ell n2\cdot(\epsilon-\nu_r)^2/\gamma_D^2]\,d\epsilon \tag{3}$$

where the usual symbols are used for the familiar physical constants. Further, μ is the absorption index, f_r and ν_r are the total integrated oscillator strength of the particular doublet component and the corresponding resonance transition frequency, respectively; and γ_L and γ_D are the Lorentzian and Doppler "full-halfwidths" (full width at half maximum). The Doppler value is

$$\gamma_D=2\frac{\nu_r}{c}\sqrt{\frac{2kT}{M}}\sqrt{\ell n2} \tag{4}$$

while the Lorentzian value is the sum of natural and collision widths

$$\gamma_L=\gamma_n+\gamma_c \tag{5}$$

Recent measurements of sodium self-broadening over the number density range $N\sim 10^{16}$ to 10^{22} (atoms/m^3) have given the values for the proportionality constant C_r in the relation

$$\gamma_c=2C_rN$$

indicated in Table 1. Table 1 also presents values of oscillator strengths, resonant frequencies and wavelengths, and natural widths for the two sodium D-lines.

By use of dimensionless variables

$$u=\frac{2\sqrt{\ell n2}(\nu-\nu_r)}{\gamma_D} \tag{6a}$$

$$a=\frac{\gamma_L}{\gamma_D}\sqrt{\ell n2}\ \text{(Voigt parameter)} \tag{6b}$$

$$y=\frac{2\sqrt{\ell n2}(\epsilon-\nu_r)}{\gamma_D} \tag{6c}$$

Table 1 Sodium D-lines parameters[a]

	λ_r, Å	ν_r, 10^{14}/s (Ref. 7)	f_r (Ref. 8)	γ_n, 10^6/s (Ref. 8)	C_r, 10^{-15} m^3/s (Ref. 9)
D_1	5895.930	5.083345	0.327	9.99	7.32
D_2	5889.963	5.088500	0.655	10.03	8.59

[a]D_1 refers to the $^2S_{1/2}\rightarrow{}^2P_{1/2}$ transition, whereas D_2 refers to the $^2S_{1/2}\rightarrow{}^2P_{3/2}$ transition.

Received April 18, 1978; revision received June 12, 1978.

Index categories: Experimental Methods of Diagnostics; Lasers.

*Research Assistant, Dept. of Aeronautics and Astronautics. Student Member AIAA.

†Professor, Dept. of Aeronautics and Astronautics. Fellow AIAA.

‡Professor, Department of Chemistry.